Modified generalised hard sphere collision model for DSMC calculations

Michael N. Macrossan*

and

Charles R. Lilley†

October 11, 2002

1. **Corresponding author:** Charles R. Lilley, Centre for Hypersonics, School of Engineering, The University of Queensland, St. Lucia, 4072, Australia.

Ph: +61 (0)7 3365 3585

Fax: +61 (0)7 3365 4799

E-Mail: c.lilley@mailbox.uq.edu.au

*Senior Lecturer, Member AIAA, Centre for Hypersonics, School of Engineering, The University of Queensland, St. Lucia, 4072, Australia. Ph: +61 (0)7 3365 4513, Fax: +61 (0)7 3365 4799, E-Mail: m.macrossan@uq.edu.au.

†PhD Research Student, Student Member AIAA, Centre for Hypersonics, School of Engineering, The University of Queensland, St. Lucia, 4072, Australia. Ph: +61 (0)7 3365 3585, Fax: +61 (0)7 3365 4799, E-Mail: c.lilley@mailbox.uq.edu.au.

Introduction

In the direct simulation Monte Carlo (DSMC) technique for modelling rarefied gas flows [1], collision cross-sections are typically determined using phenomenological molecular models. The most common DSMC molecular model is the variable hard sphere (VHS) model, described by Bird [1], where the total collision cross-section σ is given by $\sigma \propto g^{-2\upsilon}$, where g is the relative speed in collisions and υ is a constant characteristic of the gas. The VHS model has the same variation of viscosity cross-section σ_μ with relative speed as the inverse power repulsive intermolecular potential, but with hard sphere scattering. Consequently, the VHS model gives a power law viscosity relation $\mu \propto T^{\upsilon+\frac{1}{2}}$ which is inaccurate for most gases over extended temperature ranges with $T \lesssim 1000$ K.

The generalised hard sphere (GHS) model, introduced by Hassan and Hash [2], is an extension of the VHS model to include terms that allow modelling of molecules with both repulsive and attractive potentials. For the GHS model, σ may be written as

$$\sigma = \sum_{i}^{N} \sigma_i \left(g_r/g\right)^{2\upsilon_i},$$

where $g_r = (4RT_r)^{\frac{1}{2}}$ and T_r is an arbitrary reference temperature. Although any number of terms N may be used, the present analysis is limited to $N = 2$. Using $\sigma_r = \sigma_1 + \sigma_2$ and $\sigma_1 = \phi\sigma_r$, the GHS cross-section is described by

$$\hat{\sigma} = \phi\hat{g}^{-2\upsilon_1} + (1-\phi)\hat{g}^{-2\upsilon_2},$$

where $\hat{\sigma} = \sigma/\sigma_r$ and $\hat{g} = g/g_r$ are the normalised cross-section and relative speed respectively. Values of the constants σ_r, ϕ, υ_1 and υ_2 are determined using viscosity data.

The GHS model can represent the viscosity behaviour of gases more accurately than the VHS model over temperature ranges with $T \lesssim 1000$ K, where attractive intermolecular forces have a significant influence. Despite this advantage, only one DSMC study using the GHS model appears in the refereed literature (Hash, Moss and Hassan [3]). The DSMC model proposed by Kuščer [4] produces a Sutherland viscosity relation, and may be considered as a special case of the GHS model. Boyd [5] noted that σ for this Sutherland model approached infinity as $g \to 0$, but did not make any specific comments regarding computational efficiency. It appears that the GHS model is not used because of its poor computational efficiency. Here we examine the reasons for this poor computational efficiency, and introduce a modification to the model that offers significant improvements in computational efficiency with minimal effects on the viscosity behaviour.

Viscosity and collision frequency for the GHS model

The Chapman-Enskog viscosity for a given viscosity cross-section σ_μ is

$$\mu = \frac{5m}{8}\frac{(\pi RT)^{\frac{1}{2}}}{\Omega(\hat{T})}$$

where

$$\Omega(\hat{T}) = \int_0^\infty \gamma^7 \sigma_\mu \exp\left(-\gamma^2\right) d\gamma.$$

Here, $\gamma = g/(4RT)^{\frac{1}{2}}$ is a non-dimensional collision speed. For hard sphere scattering, $\sigma_\mu = 2\sigma/3$. It can be shown that $\Omega(\hat{T})$ for the GHS model is

$$\Omega(\hat{T}) = (\sigma_r/3)\left[\phi\hat{T}^{-\upsilon_1}\Gamma(4-\upsilon_1) + (1-\phi)\hat{T}^{-\upsilon_2}\Gamma(4-\upsilon_2)\right],$$

where $\hat{T} = T/T_r$ is the normalised temperature. The reference cross-section σ_r for Ar can be obtained by using the viscosity $\mu_r = 2.283 \times 10^{-5}$ Pa.s at the reference temperature $T_r = 300$ K [6], and $\sigma_r = 6.425 \times 10^{-19}$ m^2. The remaining three model parameters $(\phi, \upsilon_1, \upsilon_2) = (0.61, \frac{2}{13}, \frac{14}{13})$ give a reasonable fit to the best available viscosity data for Ar recommended by Kestin *et al.* [6], as shown in Fig. 1. The viscosity has been presented in the reduced form $\hat{\mu}/\hat{T}^{\frac{1}{2}} \propto 1/\Omega(\hat{T})$, to accentuate small differences between the curves. Note that the GHS viscosity is unrealistically low for $T \lesssim 100$ K. This low viscosity arises from a large cross-section (and consequent high collision rate), which is one of the reasons for its poor computational efficiency.

The probability of collision between two particles with total collision cross-section σ and relative speed g is proportional to $\sigma g = V$. For the Ar model parameters, a plot of $\hat{V} = V/V_r$ versus $\hat{g}$ for the GHS model is given in Fig. 2. It is apparent that $\hat{V} \to \infty$ as $\hat{g} \to 0$. The minimum point on the curve may be denoted $(\hat{g}_{\min}, \hat{V}_{\min})$.

In DSMC simulations, N_{pairs} possible collision pairs are tested, with N_{pairs} being proportional to the maximum value of V found in the simulation, denoted $V_{\max}$. The probability of a collision occurring between a possible collision pair is given by the ratio $V/V_{\max}$. Since $V_{\max}$ becomes extremely large when tested collision pairs having $\hat{g} \ll \hat{g}_{\min}$ are found, N_{pairs} becomes extremely large, while each possible collision pair has a small probability of actually participating in a collision. This has an adverse effect on computational efficiency, particularly when the temperature is low.

The molecular collision frequency ν is given by $\nu(T, n) = n\langle\sigma g\rangle$, where $\langle\sigma g\rangle$ represents the mean value of σg over all possible collision pairs. In an equilibrium gas, the distribution of $\gamma = g/(4RT)^{\frac{1}{2}}$ is

$$f_\gamma = \left(4/\pi^{\frac{1}{2}}\right)\gamma^2 \exp\left(-\gamma^2\right),$$

from which the collision frequency for the GHS model

$$\nu_{\rm GHS} = 2nV_r \left(\hat{T}/\pi\right)^{\frac{1}{2}} \left[\phi \hat{T}^{-\upsilon_1} \Gamma\left(2-\upsilon_1\right) + (1-\phi)\hat{T}^{-\upsilon_2}\Gamma\left(2-\upsilon_2\right)\right]$$

may be obtained, where $V_r = \sigma_r g_r$. If either υ_1 or $\upsilon_2 > \frac{1}{2}$, as in the present case, $\nu_{\rm GHS} \rightarrow \infty$ as $\hat{T} \rightarrow 0$. Fig. 3 shows the collision frequency for the GHS model, normalised with respect to the nominal collision frequency

$$\nu_{\rm Com} = 1/\tau_{\rm Com} = (4/\pi)\left(\rho RT/\mu_{\rm GHS}\right),$$

where $\tau_{\rm Com}$ is the nominal time between collisions. The collision frequency for the VHS model, where the viscosity is matched to the GHS viscosity, is given by

$$\nu_{\rm VHS} = \frac{15}{2(2-\upsilon)(3-\upsilon)} \frac{\rho RT}{\mu_{\rm GHS}}.$$

For Ar at high temperatures, $\upsilon = 0.22$, so $\nu_{\rm VHS}/\nu_{\rm Com} = 1.1904$, as shown in Fig. 3.

The modified GHS model

If the GHS model is modified such that $\hat{V}$ is limited at low $\hat{g}$, the computational efficiency of the model will be improved. In this analysis, the curve of $\hat{V}$ versus $\hat{g}$ for the GHS model will be modified below a transition point $(\hat{V}^*, \hat{g}^*)$ on the curve with $\hat{g}^* \leq \hat{g}_{\rm min}$. The modification will be linear, such that a finite value of $\hat{V}$ is obtained when $\hat{g} = 0$. The gradient $\alpha = d\hat{V}/d\hat{g}$ of the linear portion may be set equal to the tangent to the curve at the transition point, given by

$$\alpha = \phi(1-2\upsilon_1)\hat{g}^{-2\upsilon_1} + (1-\phi)(1-2\upsilon_2)\hat{g}^{-2\upsilon_2}, \tag{1}$$

so that the $d\hat{V}/d\hat{g}$ is continuous. Alternatively, for simplicity, $\alpha = 0$ could be used.

The equation of the modified portion of the GHS model is described by the line

$$\hat{V} = \alpha\left(\hat{g} - \hat{g}^*\right) + \hat{V}^*, \quad \text{which gives} \quad \hat{\sigma} = \alpha + (1/\hat{g})\left(\hat{V}^* - \alpha\hat{g}^*\right).$$

The modified GHS (MGHS) cross-section is then given by

$$\hat{\sigma} = \begin{cases} \alpha + (1/\hat{g})\left(\hat{V}^* - \alpha\hat{g}^*\right) & \text{when } \hat{g} \leq \hat{g}^*, \\ \phi\hat{g}^{-2\upsilon_1} + (1-\phi)\hat{g}^{-2\upsilon_2} & \text{when } \hat{g} > \hat{g}^*. \end{cases}$$

Two possibilities for the MGHS model are illustrated in Fig. 2; $\hat{g}^* = \hat{g}_{\min}$ with $\alpha = 0$, and $\hat{g}^* = \hat{g}_{\min}/2$ with α set to the gradient as given in Eq. 1. Only the first possibility is examined here.

For the MGHS model it may shown, after considerable calculus and algebraic manipulation, that

$$\Omega(\hat{T}) = (2\sigma_r/3)\left[A(\hat{T}) + B(\hat{T})\right],$$

where

$$A(\hat{T}) = \alpha\left[I_7(0) - I_7(a)\right] + \hat{T}^{-\frac{1}{2}}\left(\hat{V}^* - \alpha\hat{g}^*\right)\left[I_6(0) - I_6(a)\right], \tag{2}$$

$$2B(\hat{T}) = \phi\hat{T}^{-\upsilon_1}\Gamma\left(4-\upsilon_1, a^2\right) + (1-\phi)\hat{T}^{-\upsilon_2}\Gamma\left(4-\upsilon_2, a^2\right),$$

$$I_n(a) = \int_a^\infty \gamma^n \exp\left(\gamma^2\right) d\gamma, \quad \text{where } n \text{ is an integer and}$$

$$\Gamma(j,\beta) = \int_\beta^\infty x^{j-1}\exp(-x)dx.$$

$\Gamma(j,\beta)$ is the incomplete gamma function, and $a = \hat{g}^*/\hat{T}^{\frac{1}{2}}$. Algebraic expressions for the I_n terms that appear in Eq. 2 are given in the Appendix. The MGHS viscosity is plotted in Fig. 1. At $T \approx 100$ K, $\mu_{\rm MGHS}/\mu_{\rm GHS} \approx 1.025$. This ratio decreases rapidly at higher T. At very low T, it is apparent that the MGHS model gives a viscosity closer to the recommendations of Kestin *et al.* [6] than the GHS model. This suggests that the assumption of a finite collision probability at $g = 0$ is more realistic than the infinite value given by the GHS model.

The collision frequency of the MGHS model $\nu_{\rm MGHS} = n\langle\sigma g\rangle$ may be evaluated, again with considerable calculus and algebraic manipulation, and is given by

$$\nu_{\rm MGHS} = 4nV_r\left(\hat{T}/\pi\right)^{\frac{1}{2}}\left[C(\hat{T}) + D(\hat{T})\right],$$

where C and D are similar in form to A and B respectively, and are given by

$$C(\hat{T}) = \alpha\left[I_3(0) - I_3(a)\right] + \hat{T}^{-\frac{1}{2}}\left(\hat{V}^* - \alpha\hat{g}^*\right)\left[I_2(a) - I_2(a)\right] \quad \text{and} \tag{3}$$

$$2D(\hat{T}) = \phi\hat{T}^{-\upsilon_1}\Gamma\left(2-\upsilon_1, a^2\right) + (1-\phi)\hat{T}^{-\upsilon_2}\Gamma\left(2-\upsilon_2, a^2\right).$$

The ratio $\nu_{\rm MGHS}/\nu_{\rm Com}$ versus $\hat{T}$ is shown in Fig. 3. It is apparent that $\nu_{\rm MGHS}$ is considerably lower than $\nu_{\rm GHS}$ for $\hat{T} \lesssim 1$.

Computational efficiency

A zero-dimensional MATLAB code was used to examine the computational efficiency of the GHS and MGHS models under conditions of thermal equilibrium. DSMC simulations were performed for a set of 1000 monatomic simulator molecules for a time of $100\tau_{\rm Com}$. The simulation time step $\Delta t = 0.4\tau_{\rm Com}$. Temperatures of 100 K, 300 K and 3000 K were simulated. At each time step, the number of collision pairs tested, and the actual number of collisions performed were recorded. Simulations were also performed using the VHS model, with $\upsilon = 0.22$. The number of collisions per simulator particle per time $\tau_{\rm Com}$ is independent of temperature for the VHS model. A single simulation was therefore sufficient to establish the computational efficiency of the VHS model.

The mean results from the second half of each simulation are summarised in Table 1. The results are subject to statistical scatter, but clearly demonstrate the poor computational efficiency of the GHS model, even at high temperatures. This poor computational efficiency is due to both the higher collision frequency, and the very high number of collision pairs that are tested at each time step, due to very large values of $V_{\rm max}$. The MGHS model requires no more than 15% extra computation time than the VHS model.

In DSMC simulations, as more collision pairs are tested, the probability of finding a larger value of $V_{\rm max}$ increases. Consider a fraction of possible collision pairs δ. The expected maximum value of collision speed g after $1/\delta$ collision tests is given by the mean value of g greater than g', where a fraction δ of all possible collision pairs have $g > g'$. For an equilibrium distribution of g, the expected maximum value of g, denoted $\langle g_{\rm max}\rangle$, is given by

$$\frac{\langle g_{\rm max}\rangle}{(4RT)^{\frac{1}{2}}} = \langle \gamma_{\rm max}\rangle = \frac{1}{\delta}\int_{\gamma'}^{\infty} \gamma f_\gamma d\gamma = \frac{2}{\pi^{\frac{1}{2}}\delta}\exp\left(-\gamma'^2\right)\left(1+\gamma'^2\right),$$

where $\gamma' = g'/(4RT)^{\frac{1}{2}}$ satisfies the expression

$$\delta = \int_{\gamma'}^{\infty} f_\gamma d\gamma = 1 - \mathrm{erf}\,\gamma' + \left(2/\pi^{\frac{1}{2}}\right)\gamma'\exp\left(-\gamma'^2\right).$$

Similarly, the expected minimum value of g after a total of $1/\delta$ collision tests, denoted $\langle g_{\rm min}\rangle$, is given by

$$\frac{\langle g_{\rm min}\rangle}{(4RT)^{\frac{1}{2}}} = \langle \gamma_{\rm min}\rangle = \frac{1}{1-\delta}\int_{0}^{\gamma'} \gamma f_\gamma d\gamma = \frac{2}{\pi^{\frac{1}{2}}(1-\delta)}\left[1-\exp\left(-\gamma'^2\right)\left(1+\gamma'^2\right)\right].$$

For the GHS model, $\langle g_{\rm min}\rangle$ will provide the expected value of $V_{\rm max}$, denoted $\langle V_{\rm max}\rangle$, whereas for the MGHS and VHS models, $\langle g_{\rm max}\rangle$ will give $\langle V_{\rm max}\rangle$. For $T = 300$ K, $\langle V_{\rm max}\rangle$ versus $1/\delta$ is shown for each model in Fig. 4. For the GHS model, it is clear that $\langle V_{\rm max}\rangle$ will increase more rapidly than for either the MGHS or VHS models. The increase in $\langle V_{\rm max}\rangle$ for the MGHS model is slightly lower than for

the VHS model. It is interesting to note that $\langle V_{\max} \rangle$ will increase indefinitely during a simulation for all models, giving a decrease in computational efficiency over time if nothing is done to limit $\langle V_{\max} \rangle$.

Conclusions

The generalised hard sphere model can be modified to limit the collision probability at low collision speeds. Compared to the original model, the modification gives significant improvements in computational efficiency, both because the theoretical collision rate is lower, and because the number of possible collision partners that must be tested is dramatically reduced. The modified model requires no more than 15% extra computational time than the variable hard sphere model. For a temperature of about 100 K, the difference in viscosity between the modified version of the model and the original model is less than 2.5%, and this difference decreases rapidly as temperature increases. The modified model gives a viscosity in better agreement with recommended viscosity values than the original model for argon. This modified generalised hard sphere model can therefore be used in DSMC simulations where, in order to obtain realistic viscosity behaviour, it is necessary to model the attractive portion of the intermolecular potential.

References

[1] Bird, G. A., *Molecular Gas Dynamics and the Direct Simulation of Gas Flows*, Oxford University Press Inc., New York, 1994.

[2] Hassan, H. A. and Hash, D. B., "A Generalized Hard-Sphere Model for Monte Carlo Simulation", *Phys. Fluids A*, Vol. 5, No. 3, 1993, pp. 738–44.

[3] Hash, D. B., Moss, J. N. and Hassan, H. A., "Direct Simulation of Diatomic Gases Using the Generalized Hard Sphere Model", *J. Thermophys. Heat Tr.*, Vol. 8, No. 4, 1994, pp. 758–64.

[4] Kuščer, I., "A Model for Rotational Energy Exchange in Polyatomic Gases", *Physica A*, Vol. 158, 1989, pp. 784–800.

[5] Boyd, I. D., "Temperature Dependence of Rotational Relaxation in Shock Waves of Nitrogen", *J. Fluid Mech.*, Vol. 246, 1993, pp. 343–60.

[6] Kestin, J., Knierim, K., Mason, E. A., Najafi, B., Ro, S. T. and Waldman, M., "Equilibrium and Transport Properties of the Noble Gases and their Mixtures at Low Density", *J. Phys. Chem. Ref. Data*, Vol. 13, No. 1, 1984, pp. 229–303.

Appendix

The I_n terms that appear in Eqs. 2 and 3 have been evaluated from the general equations given by Bird [1], and are

$$
\begin{aligned}
I_2(a) &= \frac{\pi^{\frac{1}{2}}}{4}\operatorname{erfc} a + \frac{a\exp\left(-a^2\right)}{2}, \\
I_3(a) &= \frac{\exp\left(-a^2\right)}{2}\left(1+a^2\right), \\
I_6(a) &= \frac{15\pi^{\frac{1}{2}}}{16}\operatorname{erfc} a + a\exp\left(-a^2\right)\left(\frac{15}{8}+\frac{5}{4}a^2+\frac{1}{2}a^4\right) \quad \text{and} \\
I_7(a) &= \frac{\exp\left(-a^2\right)}{2}\left(6+6a^2+3a^4+a^6\right).
\end{aligned}
$$

Model	T (K)	Tests performed per τ_{Com} per simulator	Collisions performed per τ_{Com} per simulator	Acceptance rate	Theoretical collisions per τ_{Com} per simulator	CPU time relative to VHS CPU time
GHS	100	1022	2.009	0.197%	1.997	83.5
GHS	300	247.4	1.547	0.625%	1.547	24.3
GHS	3000	17.76	1.200	6.76%	1.182	2.29
MGHS	100	1.804	1.551	86.0%	1.556	1.14
MGHS	300	2.232	1.430	64.0%	1.435	1.15
MGHS	3000	2.487	1.160	46.7%	1.180	1.02
VHS	–	2.390	1.201	50.3%	1.190	1

Table 1: Summary of collision rates and computational efficiency.

List of Figures

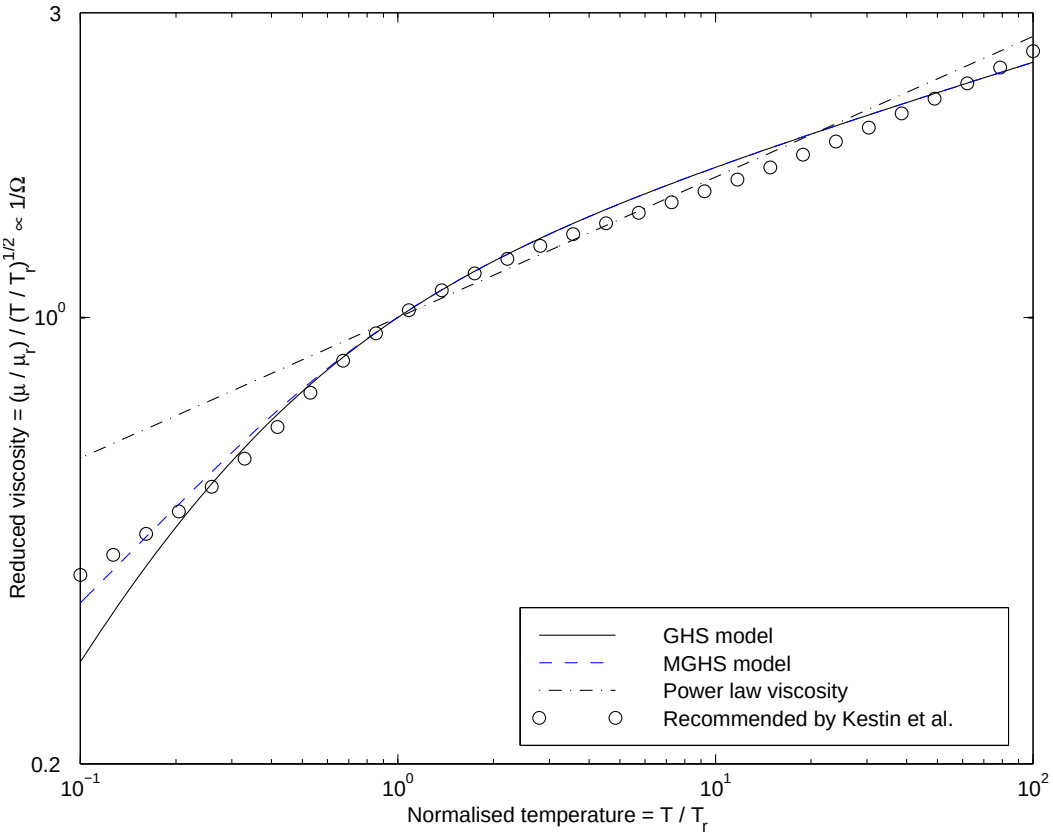

Figure 1: Macrossan and Lilley

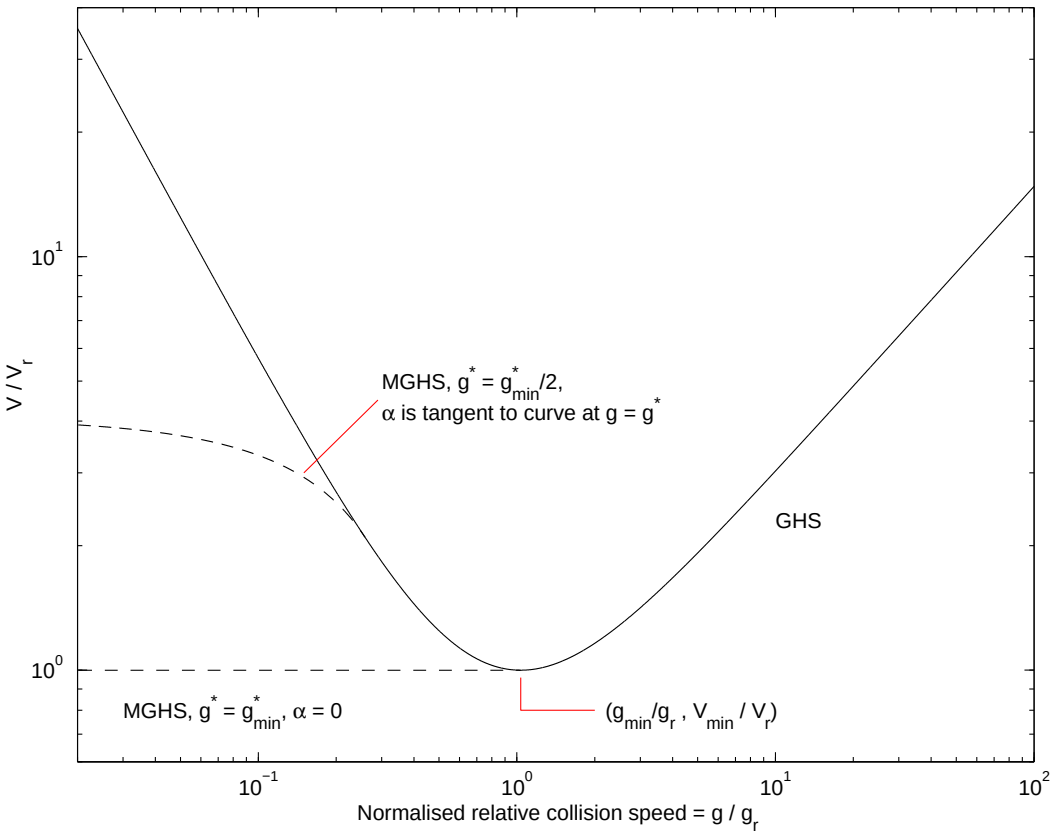

Figure 2: Macrossan and Lilley

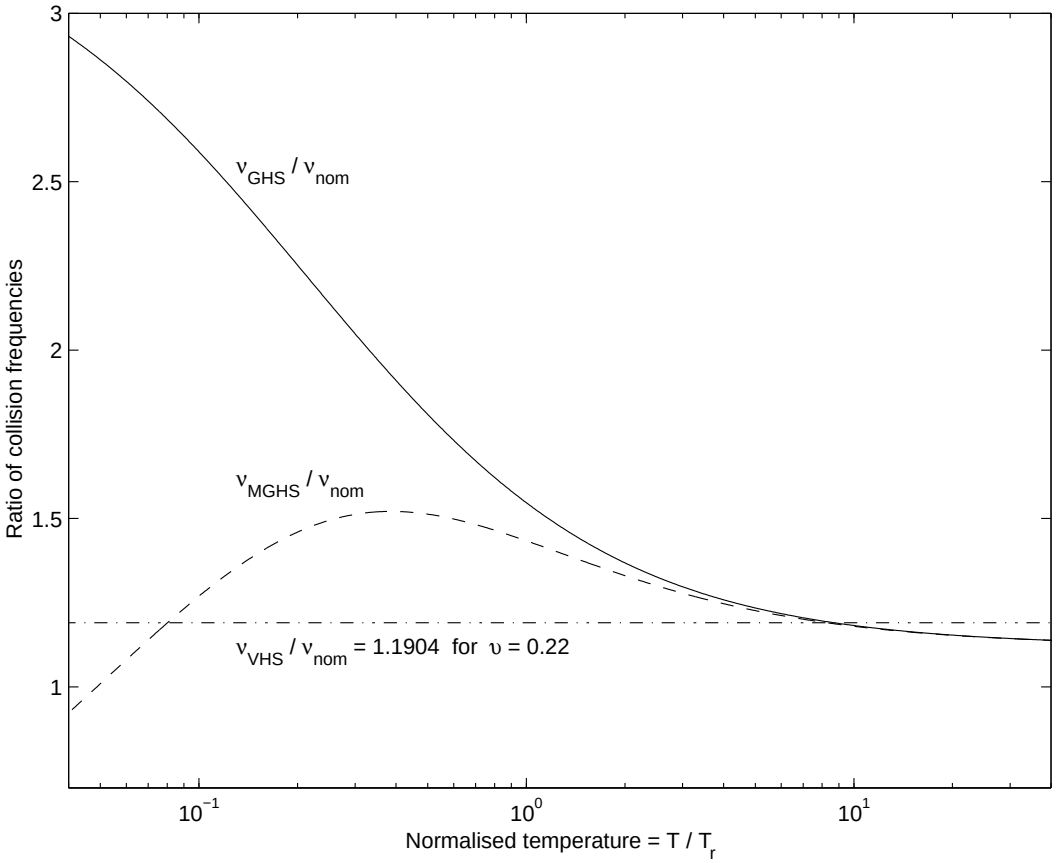

Figure 3: Macrossan and Lilley

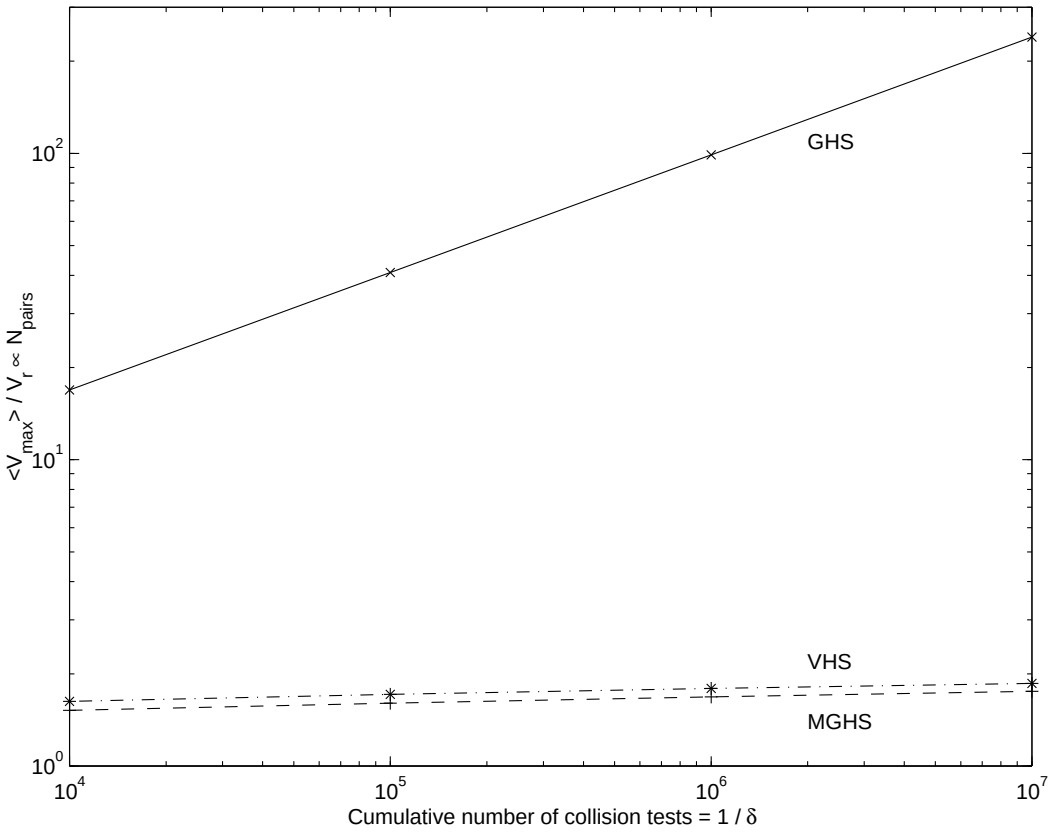

Figure 4: Macrossan and Lilley